Silicene: Compelling Experimental Evidence for Graphenelike Two-Dimensional Silicon

Patrick Vogt,[1,2,*] Paola De Padova,[3,†] Claudio Quaresima,[1] Jose Avila,[4] Emmanouil Frantzeskakis,[4] Maria Carmen Asensio,[4] Andrea Resta,[1] Bénédicte Ealet,[1] and Guy Le Lay[1,3]

[1]*Aix-Marseille University, CNRS-CINaM, Campus de Luminy, Case 913, 13288, Marseille Cedex 09, France*
[2]*Technische Universität Berlin, Institut für Festkörperphysik, Hardenbergstrasse 36, 10623 Berlin, Germany*
[3]*CNR-ISM, via Fosso del Cavaliere 100, Rome, Italy*
[4]*Synchrotron SOLEIL, Saint Aubin, BP 48 91192 Gif-sur-Yvette, France*

(Received 28 December 2011; published 12 April 2012)

Because of its unique physical properties, graphene, a 2D honeycomb arrangement of carbon atoms, has attracted tremendous attention. Silicene, the graphene equivalent for silicon, could follow this trend, opening new perspectives for applications, especially due to its compatibility with Si-based electronics. Silicene has been theoretically predicted as a buckled honeycomb arrangement of Si atoms and having an electronic dispersion resembling that of relativistic Dirac fermions. Here we provide compelling evidence, from both structural and electronic properties, for the synthesis of epitaxial silicene sheets on a silver (111) substrate, through the combination of scanning tunneling microscopy and angular-resolved photoemission spectroscopy in conjunction with calculations based on density functional theory.

DOI: 10.1103/PhysRevLett.108.155501 PACS numbers: 61.46.−w, 61.48.Gh, 81.07.−b

Since the discovery of graphene and the tremendous advancement in this field of research [1], strong effort has been invested to search theoretically and experimentally for similar two-dimensional (2D) materials composed of group-IV elements, especially silicon. The silicon equivalent of graphene was first mentioned in a theoretical study by Takeda and Shiraishi [2] in 1994 and then reinvestigated by Guzman-Verri *et al.* in 2007, who named it silicene [3]. However, silicene does not seem to exist in nature nor is there any solid phase of silicon similar to graphite. As a consequence, pure 2D silicene layers cannot be generated by exfoliation methods as performed initially in the case of graphene. More sophisticated methods have to be considered for the growth or synthesis of silicene. One promising concept for synthesizing silicene is to deposit silicon on metal surfaces that do not interact strongly with the Si atoms or form compounds. In recent years, Ag surfaces have been used to grow Si superstructures on the Ag(001) plane and to grow massively parallel Si nanoribbons on Ag(110) [4–6]. These nanoribbons were shown to be composed of hexagonal honeycomblike Si-based unit cells in agreement with density functional theory (DFT) calculations and have a linear electronic dispersion similar to massless relativistic Dirac fermions, which can be seen as a first evidence of a local silicenelike arrangement with sp^2-like hybridized Si atoms [7,8]. In order to grow real two-dimensional silicene sheets, Ag(111) surfaces with sixfold top-layer symmetry can be utilized that might support the formation of a honeycomb Si adlayer.

One important question in this context is how the synthesis and thus the existence of two-dimensional silicene can be proven incontrovertibly. Clearly, this proof is possible only if different structural and electronic aspects can be confirmed by combining different complementary experimental and theoretical methods. In particular, silicene should share essentially the same electronic properties as graphene, namely, an electronic dispersion resembling that of relativistic Dirac fermions at the $\bar{K}$ points of the Brillouin zone, the so-called Dirac points [9,10]. Furthermore, at variance with graphene, which is flat, silicene is conjectured to have a buckled honeycomb atomic arrangement of sp^3/sp^2-like hybridized Si atoms. For the nearest-neighbor Si-Si distance within this honeycomb structure of freestanding silicene, Cahangirov *et al.* found a value of 0.225 nm [9], based on DFT calculations while Houssa *et al.* reported a value of 0.226 nm [11]. These values are very close to the Si-Si distance of 0.224 nm observed for one-dimensional (1D) Si nanoribbons [5] and just slightly smaller (by 5%) than the distance in bulk silicon (0.235 nm). It is therefore reasonable to assume that the Si-Si distance should be found between 0.22 and 0.24 nm. In addition to the structural properties (honeycomb arrangement, correct Si-Si distance), a conclusive identification of 2D silicene layers has to include certain electronic properties, in particular, a linear dispersion at the silicene $\bar{K}$ point.

In a recent publication by Lalmi *et al.*, the synthesis of 2D silicene on Ag(111) was claimed based on STM observations only [12]. Because no other complementary experimental results are presented, however, the conclusion of the silicene synthesis must still be regarded as rather speculative. Moreover, the Si-Si distance determined by Lalmi *et al.* is 0.19 nm (± 0.01 nm), a value far too small compared to the expected value between 0.22 and 0.24 nm and the DFT calculations by Cheng *et al.* [13]. In addition, we have not been able to reproduce the STM results for Si/Ag(111) reported by Lalmi *et al.* nor to

obtain a similar 2D Si structure. Note that the pure Ag(111)-(1 × 1) surface can mimic a honeycomblike appearance in STM caused by a tip-induced contrast reversal, which looks very similar to the STM images reported by Lalmi *et al.* [12]. Since any chemical analysis is missing, e.g., by Auger-electron spectroscopy, we believe that the measurements presented by Lalmi *et al.* refer to clean Ag(111) only. A clear proof for the existence of 2D silicene layers, supported by complementary experimental evidence, has therefore not yet been presented.

In our work, we have studied one-atom-thick Si sheets formed on the Ag(111) surface. Clean and well-ordered Ag(111) surfaces were prepared by Ar^+ bombardment (1.5 kV, 5×10^{-5} mbar) and subsequent annealing at ≈ 530 °C for 30 min. of (111)-oriented Ag single crystals under ultrahigh vacuum conditions. Si was deposited by evaporation from a Si source consisting of a directly heated Si-wafer piece, while the Ag sample was kept at temperatures between ≈ 220–260 °C. STM measurements were performed at room temperature in constant-current mode using an Omicron VT-STM with an electrochemically etched tungsten tip. All images were drift corrected and calibrated with respect to the well-known Ag(111)-(1 × 1) surface. Angular-resolved photoelectron spectroscopy (ARPES) measurements were carried out at the ANTARES and VUV beam lines of the synchrotron radiation facilities SOLEIL (Paris, France) and ELETTRA (Trieste, Italy), equipped with hemispherical energy analyzers (Scienta). Electron-energy distribution curves were recorded along the $\bar{\Gamma}$-$\bar{K}$ direction of the Ag surface Brillouin zone (BZ) through the Si $\bar{K}/\bar{K}'$ point of the (4×4) Si adlayer. According to the relative orientation of the Ag (1 × 1) unit cell and the (4 × 4) Si adlayer, the Si $\bar{K}$ point is located at 3/4 of the Ag $\bar{\Gamma}$-$\bar{K}$ distance. The theoretical data are based on DFT as implemented in the Vienna *ab initio* simulation package (VASP) within the framework of the projector augmented wave method [14–18]. Exchange-correlation interactions are included within the generalized gradient approximation in the Perdew-Burker-Ernzerhof form [19]. The electron-ion interaction is described by the projector augmented wave method in its implementation by Kresse and Joubert [20]. A plane-wave energy cutoff of 250 eV was used for all calculations and is found to be sufficient for this system. The bulk lattice constant of 0.4175 nm was found for Ag by using a *k*-point mesh of (10 × 10 × 10). The slab supercell approach with periodic boundaries is employed to model the surface with the Brillouin-zone sampling based on the technique devised by Monkhorst and Pack [21]. The slab consists of five layers of Ag(111), each containing 16 atoms. In all our calculations we used a *k*-points mesh of (3 × 3 × 1). To confirm the accuracy of our DFT calculation, we also converged a layer of freestanding silicene giving a buckling of 0.044 nm and an Si bond angle of 116.5°. The results are in agreement with previous results [9].

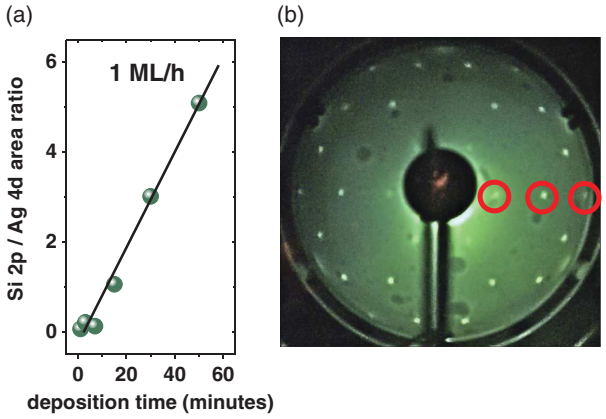

FIG. 1 (color). Growth of Si on Ag(111)-(1 × 1). (a) Area ratio between the Si 2*p* and Ag 4*d* core level emission as a function of the Si deposition time. (b) (4 × 4) LEED pattern (27 eV) after deposition of ≈ 1 ML of Si at a temperature of 220 °C. [The circles indicate the (0, $\frac{1}{4}$), (0, $\frac{1}{2}$), and (0, $\frac{3}{4}$) spots; integer order spots are outside the screen].

The growth mode of the Si adlayer was determined by measuring the area ratio between the Si 2*p* core level and the Ag 4*d* band emission as a function of the Si deposition time [Fig. 1(a)]. Clearly, the Si/Ag area ratio changes linearly, indicating an initial 2D growth behavior with a corresponding deposition rate of 1 monolayer/hr (ML/hr). After the incremental deposition steps, a (4 × 4) symmetry with respect to the bare unreconstructed Ag(111)-(1 × 1) surface can be observed by low-energy electron diffraction (LEED) with increasingly intense and sharp diffraction spots [Fig. 1(b)]. The STM topograph in Fig. 2(a) shows the Si adlayer after a deposition of approximately 1 ML.

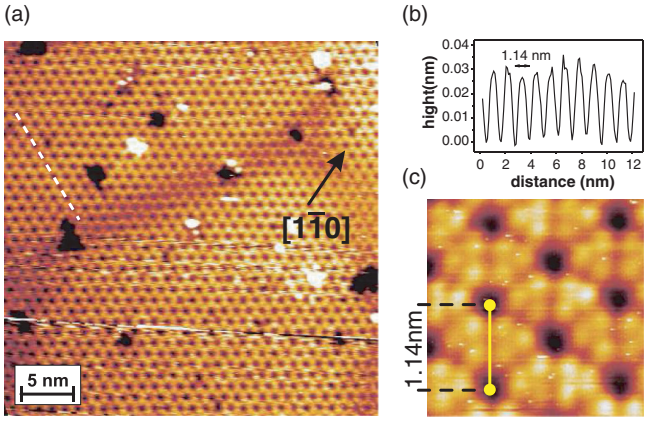

FIG. 2 (color). (a) Filled-states STM image of the 2D Si layer on Ag(111)-(1 × 1) ($U_{bias} = -1.3$ V, $I = 0.35$ nA). Clearly visible is the honeycomblike structure. (b) Line profile along the dashed white line indicated in (a). The dark centers in the STM micrograph are separated by 1.14 nm, corresponding to 4 times the Ag(111) lattice constant, in agreement with the (4 × 4) symmetry. (c) High-resolution STM topograph (3 × 3 nm, $U_{bias} = -1.3$ V, $I = 0.35$ nA) of the Si adlayer.

The image reveals an Si adlayer covering the surface terraces with a honeycomb appearance. This structure could be prepared reproducibly for different Si deposition amounts: For smaller amounts of Si (< 1 ML), the formation of smaller 2D Si islands is observed, which grow bigger with increasing deposition and finally cover the Ag(111) terraces completely (width $\approx$ 100–150 nm) observed in the STM scanning range. This result is in good agreement with the 2D growth mode. Line profiles (not shown) measured across the edge of an Si island on the Ag(111) surface reveal a height for the Si layer of approximately 0.1 nm, indicating the formation of a one-atom-thick 2D adlayer. However, the determined height might be underestimated since the tunneling conditions on the Si layer and the pure Ag surface are quite different. In order to validate the exact alignment of the 2D Si lattice vectors with respect to the ones of an Ag(111)-(1 × 1) surface, two STM images were recorded directly, one after the other, within the same surface area, where an incomplete 2D Si island and the pure Ag(111) surface were next to one another. Note that in both cases different tunneling conditions had to be chosen in order to obtain a good atomic resolution, i.e., $U_{\mathrm{bias}} \approx -0.2$ V, $I \approx 2.00$ nA for Ag(111) and $U_{\mathrm{bias}} \approx -1.4$ V, $I \approx 0.3$ nA for Si. The obtained Ag[$1\bar{1}0$] direction is indicated in Fig. 2(a).

The line profile in Fig. 2(b) was recorded along the line indicated in the STM image in Fig. 2(a). It shows that the dark centers in the STM micrograph are separated by an average value of 1.14 nm, corresponding to 4 times the surface Ag(111) lattice constant, in very good agreement with the (4 × 4) symmetry observed by LEED. The high-resolution STM image in Fig. 2(c) taken at a sample bias of $U_{\mathrm{bias}} = -1.3$ V shows that the 2D Si adlayer gives rise to triangular structures, each consisting of three bright protrusions, separated by 0.4 nm with respect to each other. These triangles are arranged hexagonally around the dark centers, which are separated by 4 Ag lattice constants. STM images recorded at other sample biases, ranging from $U_{\mathrm{bias}} = -1.4$ to -0.5 V and at $+0.6$ V, give rise to the same appearance, indicating that the STM image is probably dominated by geometric rather than electronic effects.

ARPES data recorded at a photon energy of $h\nu =$ 126 eV along the Ag $\bar{\Gamma}$-$\bar{K}$ direction through the Si $\bar{K}$ point in the right image of Fig. 3(a) identify a downward-dispersing conical branch of the honeycomb Si bands. Such bands were observed at different Si $\bar{K}/\bar{K}'$points of the surface BZ but not on the initial Ag(111) surface [shown in the left image of Fig. 3(a)]. A comparable dispersion is found in an energy range of ±5 eV around $h\nu = 126$ eV and for a photon energy of $h\nu = 78$ eV as in the case of Si nanoribbons on Ag(110) [5]. The dispersion is similar to the one for graphene, pointing toward the existence of Dirac fermions in the silicene band. The linear dispersion can be described by $E = \hbar v_F k$, where v_F is the

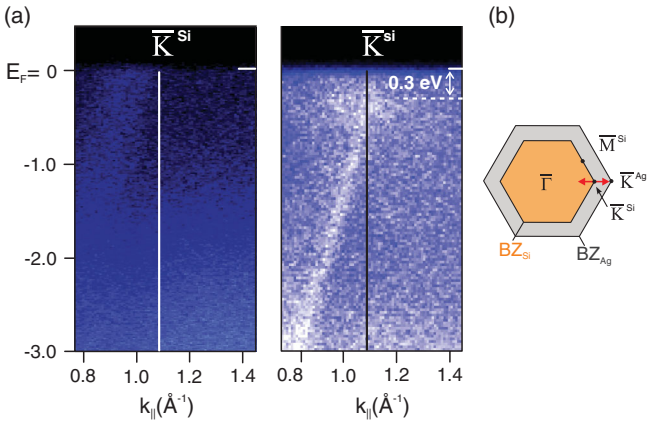

FIG. 3 (color). (a) ARPES intensity map for the clean Ag surface (left) and after formation of the 2D Si adlayer (right), taken along the Ag $\bar{\Gamma}$-$\bar{K}$ direction through the silicene $\bar{K}$($h\nu =$ 126 eV). (b) Brillouin-zone (BZ) scheme of the 2D Si layer with respect to the Ag(111)-(1 × 1) surface. The red arrow indicates the ARPES measurement direction.

Fermi velocity. From the linear dispersion in Fig. 3(b), we obtain a Fermi velocity for the silicene layer of $v_F = 1.3 \times 10^6$ ms^{-1}, comparable to the one found for graphene [22]. Similar to graphene, only a single dispersing branch of the "Dirac cone" is visible in the horizontal $\bar{\Gamma}$-$\bar{K}$ direction [Fig. 3(b) red arrow] due to a photoemission interference effect [22]. The apex of the Si cone is approximately 0.3 eV below the Fermi level. Since the π^* cone could not be detected, it can only be assumed that the gap opening between the π and π^* bands amounts to approximately 0.6 eV, as found similarly for Si nanoribbons on Ag(110) [5]. Freestanding silicene is expected to have a zero gap; however, the opening of the gap could result from an interaction with the Ag(111) substrate, an effect already observed for graphene [23].

Our data therefore show concordantly that the (4 × 4) Si adlayer in fact refers to a 2D silicene layer that is formed on the Ag(111) surface. Figure 4 shows how the STM image can be explained by such a single silicene sheet. At the top, Fig. 4(a) shows the bare Ag(111) surface, and Fig. 4(b) shows the 2D Si adlayer. This STM image is explained by a 2D honeycomb silicene sheet if the pure Si layer (bottom right) is placed on top of the Ag(111) surface (gray spheres) in such a way that (3 × 3) silicene unit cells coincide with a (4 × 4) Ag(111)-(1 × 1) area. In this case, the Si atoms are located either on top of Ag atoms (large orange spheres) or between Ag atoms (small orange spheres). In STM images [Fig. 4(b)] only the on-top atoms are visible, leading to the same triangular arrangement as depicted in the model [Fig. 4(c)], forming a (4 × 4) coincidence cell in agreement with the LEED observations. From the STM image, the in-plane Si-Si distance can be determined from the distance D of the dark centers in Fig. 2(c) according to $a = D/(3\sqrt{3})$. In this way, we obtain an average Si-Si distance

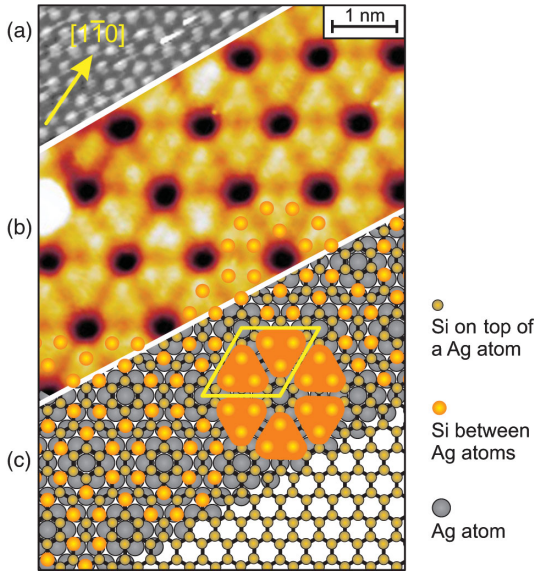

FIG. 4 (color). Construction of the atomic structure model for the 2D Si adlayer. Filled-states STM images of (a) the initial clean Ag(111)-(1 × 1) surface ($U_{bias} = -0.2$ V, $I = 1.93$ nA) and (b) the (4 × 4) silicene sheet ($U_{bias} = -1.4$ V, $I = 0.29$ nA). (c) Model of silicene on Ag(111). Si atoms sitting on top of Ag atoms are highlighted as larger orange balls, resembling the measured STM image. In the bottom right corner, the ball-and-stick model for the freestanding silicene layer is shown with an Si-Si distance of 0.22 nm.

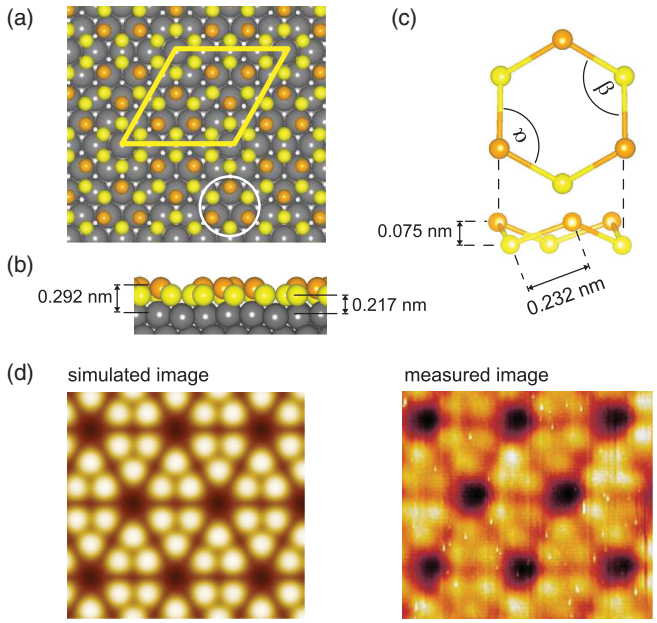

FIG. 5 (color). DFT results for the silicene on Ag(111). (a) Top view of the fully relaxed atomic geometries of the model for silicene on the Ag(111) surface from Fig. 3. (b) Side view of (a). c) Enlarged image of the hexagonal silicene ring indicated by the white circle in (a). (d) Simulated STM image (left) for the structure shown in (a). The simulated image exhibits the same structural features as those observed in the experimental STM image (right), i.e., a hexagonal arrangement of the triangular structure around dark centers.

of 0.22 nm (± 0.01 nm), in excellent agreement with the theoretical predictions for silicene [9].

In order to clarify the energetic stability of the suggested structure model, *ab initio* calculations based on DFT were performed, including full structural relaxations. These calculations reveal that the total energy for the structure model shown in Fig. 4(c) has a negative value and an adhesion energy of −0.48 eV for each Si atom, demonstrating that the silicene arrangement on Ag(111) is energetically stable. The obtained relaxed geometry is depicted in Fig. 5(a) (top view) and Fig. 5(b) (side view). It can be seen that the Si atoms of the silicene layer which are located directly on top of underlying Ag atoms are slightly displaced in z direction with respect to the bottom Si atoms. The distance between the top (bottom) Si atoms and the average height of the first Ag layer is 0.292 ± 0.002 nm and 0.217 ± 0.003 nm, respectively. As a result of this displacement, triangular structures are formed in the silicene top layer consisting of three Si atoms, which are separated by 0.38 nm. This is in very good agreement with the experimental STM observations that show the same triangular structure and a separation of approximately 0.40 nm. In Fig. 5(c), a hexagonal silicene ring from (a) [indicated by the white circle in (a)] is shown in top and side view. The theoretically determined Si-Si distance is 0.232 nm, which also agrees very well with the experimentally determined value of 0.22 nm, and top and bottom Si atoms are separated by 0.075 nm. Following these calculations, we have also determined the bond angles of the Si atoms, which also give information on the hybridization state of the respective atom. In detail, we find, for the six top Si atoms of the (4 × 4) unit cell, bond angles of ≈ 110° (α), which is very close to an angle of 109.5° for an ideally sp^3-hybridized Si atom. From the remaining 12 bottom Si atoms, six are purely sp^2 hybridized (bond angle of ≈ 120°) and six have bond angles of between ≈ 112° and ≈ 118° (β), indicating a sp^3/sp^2 hybridization. These different bond angles of the Si atoms result from the displacement of the Si atoms in z direction caused by the interaction with the Ag(111) substrate. However, most of the atoms are sp^3/sp^2 hybridized, which is probably the equilibrium state, in agreement with calculations for freestanding Si [9].

Based on the relaxed geometry, STM images were simulated by calculating the local electron density of states according to the Tersoff-Hamann approach [24]. In Fig. 5(d), it can be seen that the simulated STM image exhibits the same structural features as those observed experimentally, i.e., a hexagonal arrangement of the triangular structure around dark centers. By looking at the charge density around top and bottom Si atoms (not shown here), we find that they are electronically very similar. That means that the STM corrugation is mainly dominated by geometrical aspects rather than by electronic effect, which

is in good agreement with the voltage independence of the experimental STM images mentioned above. The DFT-based calculations therefore clearly support the suggested structure model and give evidence that the (4×4) 2D Si adlayer refers to silicene.

The STM and ARPES results demonstrate that both structural and electronic properties of the 2D Si adlayers are very similar to those for graphene and in agreement with all related expectations for silicene. This interpretation is clearly supported by DFT calculations, which agree very well in terms of the Si-Si distance, the layer height, the geometry, and the STM image. We conclude that the (4×4) 2D Si adlayer on Ag(111) is a real two-dimensional silicene sheet. The synthesis of silicene opens up interesting perspectives since silicene, with nontrivial electronic structure and a spin-orbit coupling of 1.55 meV that is much larger than that of graphene, is predicted to exhibit a quantum spin Hall effect in an accessible temperature regime [25]. Moreover, silicene can more easily be integrated into current Si-based electronics compared to graphene.

This work was financially supported within the project 2D-NANOLATTICES of the Future and Emerging Technologies (FET) program within the 7th framework program for research of the European Commission, under FET Grant No. 270749, the Deutsche Forschungsgemeinschaft (DFG) under Grant No. VO1261/3-1, and the Project for International Scientific Cooperation (PICS) under Grant No. 40237. We thank Alain Ranguis and Stephane Lorcy for their technical assistance.

*patrick.vogt@tu-berlin.de
†depadova@ism.cnr.it

[1] A. K. Geim, Science **324**, 1530 (2009).
[2] K. Takeda and K. Shiraishi, Phys. Rev. B **50**, 14916 (1994).
[3] G. G. Guzmán-Verri and L. C. Lew Yan Voon, Phys. Rev. B **76**, 075131 (2007).
[4] H. Sahaf, L. Masson, C. Léandri, B. Aufray, G. Le Lay, and F. Ronci, Appl. Phys. Lett. **90**, 263110 (2007).
[5] P. De Padova, C. Quaresima, C. Ottaviani, P. M. Sheverdyaeva, P. Moras, C. Carbone, D. Topwal, B. Olivieri, A. Kara, H. Oughaddou, B. Aufray, and G. Le Lay, Appl. Phys. Lett. **96**, 261905 (2010).
[6] P. De Padova, C. Quaresima, P. Perfetti, B. Olivieri, B. Léandri, B. Aufray, S. Vizzini, and G. Le Lay, Nano Lett. **8**, 271 (2008).
[7] A. Kara, C. Léandri, M. E. Davila, P. De Padova, B. Ealet, H. Oughaddou, B. Aufray, and G. Le Lay, J. Supercond. Novel Magnetism **22**, 259 (2009).
[8] P. De Padova, C. Quaresima, B. Olivieri, P. Perfetti, and G. Le Lay, Appl. Phys. Lett. **98**, 081909 (2011).
[9] S. S. Cahangirov, M. Topsakal, E. Aktürk, H. Şahin, and S. Ciraci, Phys. Rev. Lett. **102**, 236804 (2009).
[10] T. Suzuki and Y. Yokomizo, Physica (Amsterdam) **42E**, 2820 (2010).
[11] M. Houssa, G. Pourtois, V. V. Afanasev, and A. Stesmans, Appl. Phys. Lett. **97**, 112106 (2010).
[12] B. Lalmi, H. Oughaddou, H. Enriquez, A. Kara, S. Vizzini, B. Ealet, and B. Aufray, Appl. Phys. Lett. **97**, 223109 (2010).
[13] Y. C. Cheng, Z. Y. Zhu, and U. Schwingenschlögel, Europhys. Lett. **95**, 17005 (2011).
[14] P. Hohenberg and W. Kohn, Phys. Rev. **136**, B864 (1964).
[15] W. Kohn and L. J. Sham, Phys. Rev. **140**, A1133 (1965).
[16] G. Kresse and J. Hafner, Phys. Rev. B **47**, 558 (1993).
[17] G. Kresse and J. Furthmüller, Phys. Rev. B **54**, 11169 (1996).
[18] G. Kresse and J. Furthmüller, Comput. Mater. Sci. **6**, 15 (1996).
[19] J. P. Perdew, K. Burke, and M. Ernzerhof, Phys. Rev. Lett. **77**, 3865 (1996).
[20] G. Kresse and D. Joubert, Phys. Rev. B **59**, 1758 (1999).
[21] H. J. Monkhorst and J. D. Pack, Phys. Rev. B **13**, 5188 (1976).
[22] K. R. Knox, S. Wang, A. Morgante, D. Cvetko, A. Locatelli, T. O. Mentes, M. A. Niño, P. Kim, and R. M. Osgood, Jr., Phys. Rev. B **78**, 201408(R) (2008).
[23] S. Y. Zhou, G.-H. Gweon, A. V. Fedorov, P. N. First, W. A. de Heer, D.-H. Lee, F. Guinea, A. H. Castro Neto, and A. Lanzara, Nature Mater. **6**, 770 (2007).
[24] J. Tersoff and D. R. Hamann, Phys. Rev. B **31**, 805 (1985).
[25] C.-C. Liu, W. Feng, and Y. Yao, Phys. Rev. Lett. **107**, 076802 (2011).